PHYSICAL REVIEW B VOLUME 39, NUMBER 17 15 JUNE 1989-I

Adsorbed layer and multilayer materials: The energetics and bonding of Pd and Ag on Nb(001) and Nb(110)

M. Weinert, R. E. Watson, J. W. Davenport, and G. W. Fernando
Department of Physics, Brookhaven National Laboratory, Upton, New York 11973

(Received 7 September 1988; revised manuscript received 23 November 1988)

The energetics of transition-metal–transition-metal adlayer adhesion and the heats of formation for competing ordered compounds have been investigated using total-energy calculations in order to disentangle the factors controlling adlayer behavior. The calculated energies are used to estimate interface energies, distortion energies associated with requiring an adlayer to be commensurate with its substrate, the surface energies of the bare metal surfaces of Nb(110), Nb(001), Ag(110), Ag(001), Pd(110), and Pd(001), and the surface energies associated with the presence of an adlayer. The results provide a picture consistent with the experimentally known adlayer behavior for Pd-Nb(001), Pd-Nb(110), and Ag-Nb(110) and have implications for the growth of artificial multilayer (superlattice) materials. While Pd adsorption on Nb can already be understood in terms of bulk interface energetics, for Ag on Nb the surface contributions are essential. Densities of states obtained for bulk multilayers display markedly different bonding at the Pd-Nb and Ag-Nb interfaces, although all show a pronounced interface state ~ 1.5 eV above the Fermi level. The intensity of this peak, which also exists at the surface, reflects the strength of bonding at the interface.

I. INTRODUCTION

With the advent of new experimental techniques for adsorbing controlled amounts of atoms onto metallic substrates, interest in the properties of metal-metal interfaces has grown. From a practical point of view, it is important to learn which factors govern the growth modes. In many cases, one would like to epitaxially adsorb one metal onto another in order to modify the surface properties or to make artificial multilayer (superlattice) materials. Thus one needs to understand the physics of planar interfaces. In addition, there are many stable crystal structures, such as Au_3Nb_2 and Pd_5Ti_3, which involve planar stacking.

The purpose of the present paper is to theoretically explore the energetics and bonding of planar transition-metal systems in an attempt to gain new insight into the mechanisms of interface and multilayer formation. We use self-consistent total-energy electronic structure calculations both for bulk ordered compounds and multilayers and for surfaces with and without adlayers to discuss the interplay between bulk and surface contributions. A future paper will employ the same set of calculations to discuss quantities of spectroscopic interest, work-function trends, and localization of states at interfaces.

The Pd-Nb and Ag-Nb systems we consider are of experimental interest, but more importantly provide a juxtaposition of two different types of bulk phase diagrams. The Pd-Nb system displays strong compound formation, while the bulk phase diagram for Ag-Nb indicates completely immiscibility and no intermediate compounds. Contrary to naive expectations, neither of these types of bulk phase diagrams favor pseudomorphic growth ("wetting"). In the case of strong compound formation, one should expect compound formation also at the interface, thereby destroying the sharp interface and layer-by-layer growth. While for Ag-Nb, and the better-known Cu-Ru system, the noble metal does remain on the surface, pseudomorphic growth is still incompatible with the bulk phase diagram alone. Clearly, minimizing the contact between the different components, as required by the bulk phase diagram, is best done by forming large clusters or islands of Ag or Cu, rather than growing pseudomorphically, which in fact maximizes the contact. Hence both types of bulk phase diagrams that we are considering in this paper discourage pseudomorphic growth. Obviously, the bulk phase-diagram behavior alone is not enough to understand adlayer and multilayer formation for these systems.

Several factors contribute to the energetics of multilayer systems. Consider a crystalline substrate of element B covered with a thick epitaxial layer of element A. Using the elemental solids A and B as reference materials, the heat of adsorption for such a layer is

$$\Delta E = \gamma_A - \gamma_B + \xi + \Delta E_{\text{str}} , \tag{1}$$

where $\gamma_A - \gamma_B$ is the difference in surface energy between having a surface of element A rather than B. (In order that the solids exist, the separate surface energies $\gamma_{A,B}$ are, of course, necessarily positive.) ΔE_{str} is the structural energy, if any, in preparing A so that it lies in registry with B and ξ is the energy associated with bonding at the interface. In the case of a multilayer system, there are no free surfaces and Eq. (1) becomes

$$\Delta E = 2\xi + \Delta E_{\text{str}} . \tag{2}$$

©1989 The American Physical Society

Here a factor of 2 enters, multiplying the ξ term, since a unit cell of a multilayer system has two interfaces, $A \rightarrow B \rightarrow A$. A multilayer compound may arise where neither the A nor B strata conform to the atomic positions in elemental A and B. If so, there are then contributions to ΔE_{str} from both A and B. There is some arbitrariness when dividing up the terms in Eqs. (1) and (2). For example, should the atomic layer which is in contact with the other atomic species at the interface be taken to make a contribution to ΔE_{str} or should its entire binding (or nonbinding) energy contributions be attributed to the interface term ξ? We use calculations for the energy of the distorted elemental bulk metal compared to its stable undistorted phase to define ΔE_{str}; we then, as a rule, apply that ΔE_{str} to all planes in the multilayer (or adlayers on the surface) in order to define ξ.

In the Pd-Nb system, it has been observed experimentally[1] that Pd forms thick epitaxial layers on Nb(001) surfaces. In contrast, Pd forms[2] only a single epitaxial layer on the denser-packed Nb(110) surface, with subsequent layers of Pd lying incommensurately. As will be shown, these trends are already understood in terms of the bulk energy contributions, ξ and ΔE_{str}, alone.

Ag forms[3] several commensurate layers on top of Nb(110). In agreement with experiment and the bulk phase diagram, the calculated ξ's are positive, i.e., nonbinding. Thus, the surface terms in Eq. (1) must be responsible for the wetting of Ag on Nb. We show that the surface energy of Nb, which is a positive energy cost associated with severing bonds at the surface, is sufficiently larger than that of Ag to allow Ag to wet Nb despite the fact that the two elements resist contact with each other. The implication, of course, is that Nb resists wetting Ag substrates. Surface energies thus produce a bias when laying metal A on B and vice versa, which has serious implications for the construction of artificial multilayer materials.

The next section provides a brief discussion of the total-energy calculations and this is followed by a discussion of calculated results for ordered compounds and bulk multilayers. It will prove useful to compare the heats of formation obtained for the multilayers with those deduced for competing ordered structures. Both the energetics of the multilayer formation and the relationship to calculated charge-transfer terms and local densities of states will be considered. While care must be taken in viewing them, since any such sampling of the charge at sites is hostage to the approximations used in calculating them, such results offer insights into the bonding which is occurring. After a discussion of the calculated surface energies γ for the bare elemental metals (Nb, Ag, and Pd) and for monolayers of Ag and Pd on Nb, we consider the implications of our results for the energetics and growth modes of interface formation.

While the present calculations do not explore all the stacking possibilities, e.g., incommensurate stackings are omitted, the energy terms derived allow one to rationalize the observed behavior in the Nb-Pd and Nb-Ag systems. This suggests that similar calculations, for systems which have yet to be explored experimentally, would let one predict the gross features of their behavior.

II. CALCULATIONS

The calculations for the bulk multilayers were done employing the self-consistent, scalar relativistic, linearized augmented Slater-type-orbital (LASTO) method[4] in much the same manner as was done previously[5] for the Pt-Ta layered system. Local-density, muffin-tin potentials were used with common sets of atomic sphere radii[6] employed in different calculations whose total energies were to be compared—different sphere radii, reflecting the differences in atomic size, were used for Nb, Pd, and Ag, respectively. This class of calculation as applied to the elemental metals[7] and to compounds[8] has been described in detail elsewhere. Sets of special k points were used whose sizes were sufficient for generating densities-of-states plots. Such k samplings are somewhat larger than what is required for convergence in the total energy. In the calculations which will be reported for Pd_2Nb in various structures, the experimental molecular volume was employed, while c/a ratios and internal atomic coordinates (placing one atomic layer relative to another) were determined variationally. In the case of the Pd_xNb_x (or Ag_xNb_x) multilayers, where $x \geq 2$, the atomic spacings of the base layers were kept equal to those of Nb(001) [or (110)] so that comparison could be made with the slab calculations. Nb-Nb interlayer spacings were frozen at the values appropriate to bcc Nb while the Pd-Nb and Pd-Pd (or Ag-Nb and Ag-Ag) layer spacings were determined variationally in a calculation for Pd_2Nb_2 (or Ag_2Nb_2). The same atomic spacings were then used for the thicker multilayers, where $x > 2$.

While the use of muffin-tin potentials for close-packed elemental metals is known to be a reasonable approximation, it is perhaps less clear that interfacial energies of layered structures can be accurately calculated within this approximation. Previous comparisons between calculations[8] and experiment for compounds in various structures demonstrated that accurate heats of formation could be obtained using muffin-tin potentials for close-packed compounds, including such intrinsically layered structures as the CuAuI, $MoSi_2$, and $MoPt_2$ structures. (For open structures like the A15's with intrinsically lower symmetry, the calculated heats are in rather poor agreement with experiment.) Since the interfaces of the multilayers are neither of lower symmetry nor worse packed than these layered compounds, we would expect similarly good interfacial energies as for the heats of formation of the compounds. Furthermore, since the various energy terms that are of interest here are always calculated as *differences* of total energies, there are significant cancellations of errors. As is well known and has been documented in the literature many times, it is precisely this cancellation of errors that allows one to compare results calculated using two different computational methods and/or levels of approximations.

Full-potential linearized augmented-plane-wave calculations (FLAPW) were used for the slabs. Employing full, rather than muffin-tin, potentials implies a superior treatment of the charge density and the associated crystal potential which is crucial for the intrinsically lower symmetry associated with the surface. The calculations were done for slabs nine atomic layers thick with enough k points for an accurate determination of the total energy and density of states. A more detailed discussion of the methods may be found elsewhere.[9] For the (001) and (110) faces of bcc Nb and fcc Ag and Pd, the spacings between layers were taken to be those of the bulk up to and including the distance between the surface and subsurface layers. In addition, calculations with monolayers of Pd and Ag in registry on either side of a seven-layer slab of Nb (001) or (110) were done. The interior Nb spacings were those of bulk bcc Nb and for Pd/Nb (110), the adlayer spacing was determined variationally. The separation was somewhat less than what would have been obtained based on atomic radii if those radii were attributed to both Pd and Nb in bcc lattices at the observed atomic volume. The effect of the variations was to improve the total energy of a slab by ≤ 0.05 eV per surface atom. The Pd results were used as a basis for setting the Ag adlayer positions without any variational search.

To separate surface and bulk energies requires taking differences between several calculations. Obviously, to get meaningful numbers, it is necessary that the various calculations are done with consistent approximations and are converged with respect to calculational parameters. The required bulk and surface energies are derived from the total energies of slabs of varying thicknesses (typically seven and nine layers) assuming that the total energy for an n-layer slab of an elemental metal is given by $E_n = nE_{\text{bulk}} + 2\gamma$, where E_{bulk} is the total energy per atom in the bulk. To obtain the converged energy of an n-layer slab, a series of self-consistent calculations at various basis sizes (ranging from $|G|^2 = 10.2-16$ a.u.) was extrapolated to infinite basis size, using both exponential and power-law fits. These fits typically agreed to better than 1 mRy. A stringent consistency check on the convergence of the calculations is a comparison of E_{bulk} determined for different crystal faces of the same element, since the different geometries of the slabs yield different convergence rates with respect to basis size, etc. For the cases considered here, the agreement was within the extrapolation errors. This consistency check was a strong motivating factor, besides the intrinsic physical interest, for determining the face dependence of the surface energy. We have neglected lattice relaxations in the calculations, but since these effects are only a few percent of the surface energies, they will not change our conclusions or numbers to the precision given later.

III. RESULTS: BULK $Pd_xNb_{(1-x)}$ AND $Ag_xNb_{(1-x)}$ COMPOUNDS

Pd_2Nb is one of the stable phases of the Pd-Nb system and forms in one of several competing layered crystal structures which are closely related to the layerings of concern here. There is the familiar c/a tetragonal distortion of a fcc lattice which takes it into the bcc. This distortion[10] takes the $MoSi_2$ structure [*abb* stacking of bcc (001) planes] into the $MoPt_2$ structure [*abb* stacking of fcc (110) planes]. There is a less well-known orthorhombic distortion which takes the stacking of bcc (001) planes into a bcc (110) stacking. This is illustrated in Fig. 1. Thus one can continuously follow the energetics of the Pd_2Nb phase as a function of these distortions and address such issues as whether close-packed bcc (110) layering is favored over the less close-packed (001) in the bulk. Note there is no unique path taking one of the structures into another. On going from $MoSi_2$ to $MoPt_2$ the ratio of the z to the x lattice constant was held fixed, which corresponds to maintaining the square symmetry of (010) planes (which are square in both of the end compounds). On taking the (001) bcc stacking of the $MoSi_2$ phase into the (110) bcc stacking, y of Fig. 1—the (010) plane separation—was held fixed. This corresponds to the least movement of the atoms on going from one structure to the other.

The calculated binding energy per atom is plotted as a function of these distortions in Fig. 2. The $MoPt_2$ structure is calculated to be the most stable phase, in agreement with experiment, though more stable by only a modest amount relative to the $MoSi_2$ structure. The bcc (110) layering is significantly less stable and this is easily understood. Pd and Nb tend to form compounds, and stacking them in close-packed (110) layers minimizes the number of Pd-Nb nearest-neighbor pairs, thus minimizing the bonding to be gained. The results of Fig. 2 contrast in several subtle ways with similar results obtained previously for Pt_2Ta—the $5d$ transition-metal analog of Pd_2Nb. First, the lowest calculated energy for Pt_2Ta was obtained for a y/x, corresponding to neither the $MoPt_2$ nor the $MoSi_2$ structure but instead to a distorted structure between the two; in fact, Pt_2Ta forms in a distorted phase. Secondly, Pt_2Ta with the bcc (110) layering, unlike Pd_2Nb, was found to be locally stable though globally unstable, i.e., Pt_2Ta has a local total-energy minimum in the vicinity of bcc (110) though both the $MoSi_2$ and $MoPt_2$ structures were lower in energy. This suggests

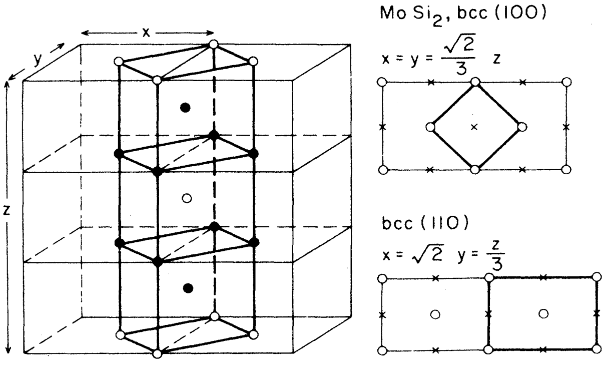
x
y
z
Mo Si$_2$, bcc (100)
$x = y = \frac{\sqrt{2}}{3} z$
bcc (110)
$x = \sqrt{2}\ y = \frac{z}{3}$

FIG. 1. To the left: a unit cell of the $MoSi_2$ structure inside a larger cell with rotated axes with a view of that cell, as seen from above, being shown to the upper right. The distortion of the larger unit cell which takes the *abb* stacking of (001) bcc planes in the $MoSi_2$ structure into an *abb* stacking of close-packed (110) layers of the bcc structure is shown in the lower right.

that a metastable $Pt_2Ta(110)$ bcc phase, once constructed, might exist while Pd_2Nb would rather easily undergo a distortion into the $MoSi_2$, and in turn, the $MoPt_2$ structure.

The open circles in Fig. 2 correspond to the binding energies of the phases where the (001) or (110) planes were required to conform to the spacing of bcc Nb: this requirement introduces a substantially larger energy cost for the (110) stacking than for the $MoSi_2$ structure.

A tracing of the phase diagram of the Pd-Nb system, as reported[11] by Moffatt, appears in Fig. 3 as do calculated heats for PdNb, Pd_2Nb, and Pd_3Nb in several assumed structures. There is not complete agreement in the literature over some of the features of the phase diagram, in particular as to whether a high-temperature PdNb phase does occur. If it does exist, its structure (although unknown) is thought to be fcc-like. The calculated heats for PdNb in the ordered CsCl and CuAuI structures lie below the line drawn between the zero for pure Nb and the heat calculated for Pd_3Nb (or Pd_2Nb). This implies that these 50%-50% phases are unstable relative to a two-phase mixture of pure Nb and Pd_3Nb (or Pd_2Nb) and this is consistent with the phase diagram. To the extent that the highest of the Pd_2Nb heats lies on or above the line drawn between Pd_3Nb and pure Nb implies that Pd_2Nb is stable relative to a two-phase mixture of the two. As already noted, Pd_2Nb is calculated to be stablest in the $MoPt_2$ structure, consistent with experiment. Similarly, Pt_3Nb is calculated to be stabler in the Al_3Ti phase than in the Cu_3Au to which it is structurally related. The Al_3Ti structure is one of two phases reported for Pd_3Nb (the other phase has too large a unit cell to be dealt with here). Thus the calculations are in accord with the phase diagram, indicating that Pd_2Nb in the $MoPt_2$ structure and Pd_3Nb in the Al_3Ti structure do exist.

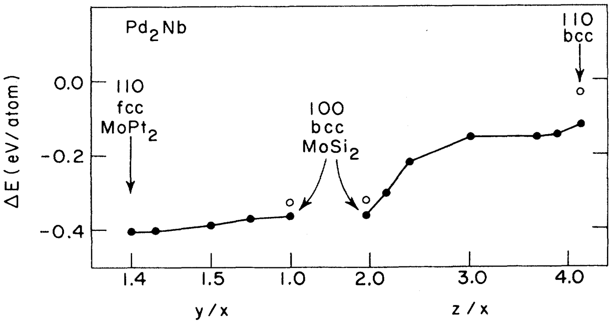

FIG. 2. Heats of formation of Pd_2Nb for distortions off the bcc-based $MoSi_2$ structure. The left-hand panel takes this structure from the bcc (001) to the fcc (110) *abb* stacking of the $MoPt_2$ structure. The right-hand panel takes the $MoSi_2$ structure with its (001) stacking to the close-packed (110) stacks, as defined in Fig. 1. Here x and z have the meaning of Fig. 1. The solid circles correspond to having the base plane dimensions as well as the layer separations of the three end points—the $MoPt_2$, $MoSi_2$, and bcc (110) structures—determined variationally while the open circles were obtained requiring the bcc (001) or (110) planes to have the dimensions characteristic of bcc Nb.

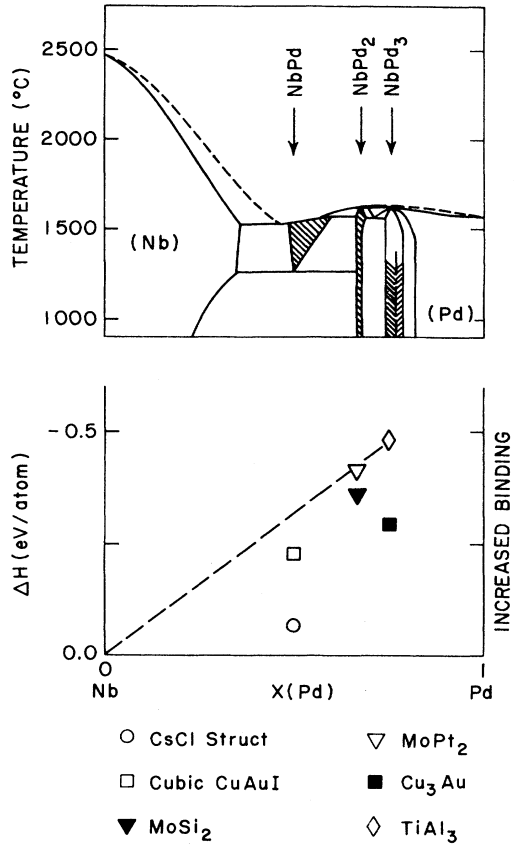

FIG. 3. A tracing of the phase diagram (Ref. 11) for the Pd_xNb_{1-x} phase diagram plus calculated heats of formation for PdNb, Pd_2Nb, and Pd_3Nb in some ordered structures. Note that the $MoPt_2$ and $TiAl_3$ structures are the observed structures at 2:1 and 3:1 compositions.

Normally one expects the largest heats of formation in an alloy sequence to occur at 50%-50% concentration, where there will be the largest number of unlike-atom nearest-neighbor pairs, which maximizes bonding. This is not the case here: consistent with many Pd and Pt alloy systems, the heat of formation per atom is larger at Pd_3Nb than at Pd_2Nb, while that for Pd_2Nb is larger than that for PdNb. Inspection of the calculated densities of states for such compounds indicates that large heats occur when alloying causes the d band of Pd or Pt (or, for that matter, Rh, Ru, Ir, etc.) to be filled so that these levels may *float free of the Fermi level,* thus increasing their effectiveness in bonding. The band filling, of course, involves the hybridization of Nb wave-function character into the predominantly Pd-like "d bands." This band filling occurs as readily for Pd_3Nb as it does for PdNb and this appears essential to the skewing of the heats in favor of the Pd-rich end. (In the split-band case of concern here, the states in the lower Pd- or Pt-like bands are obviously bonding with respect to Pd and Nb. The energy competition is then between the loss of Nb-Nb bonding versus the gain in Pd-Nb bonding. Consistent with this idea, the Fermi level for larger Nb concentrations does fall higher in the partially filled Nb-like "antibonding" bands.)

Heats for AgNb and Ag_3Nb are reported in Fig. 4. These are all nonbonding, which is consistent with the known phase-diagram behavior, and they suggest a similar skewing, though for heats of *opposite* sign, to that seen for Pd-Nb.

IV. RESULTS: Pd_xNb_x AND Ag_xNb_x MULTILAYERS

As has already been noted, the multilayers have been taken to have in-plane atomic positions which are characteristic of bcc Nb, while the *M-M* and *M*-Nb (*M* being Pd or Ag) spacings between planes are obtained variationally for the M_2Nb_2 two-on-two multilayers. The *M-M* spacings can then be employed in bulk calculations of Pd or Ag alone in order to obtain the distortion energy ΔE_{str}. For Pd, $\Delta E_{\mathrm{str}} = +0.12$ and $+0.24$ eV per atom relative to fcc Pd for Pd-Nb (001) and (110) stackings, respectively. ΔE_{str} is energetically important to the adsorption of Pd and Nb(110) while for Pd on Nb(001) it is much less significant–perhaps the best sense of energy scales is provided by noting that the competing surface energy[12] γ of liquid Nb is $\sim\frac{1}{3}$ eV per atom greater than that for liquid Pd (see Sec. V). The Pd-Pd separations imply Pd atomic volumes which are roughly one percent smaller than that of fcc Pd, i.e., volume has been approximately conserved. Pd-Nb separations of 2.788 and 4.019 a.u. were obtained for the (001) and (110), respectively. Whether these are deemed to represent chemical contractions or expansions depends on how they are viewed. If one again invokes volume, attributing to Pd a Pd-Pd spacing yielding the observed fcc Pd volume, one could take the average of this spacing and that characteristic of bcc Nb as a reference Pd-Nb distance. Doing this, one obtains that Pd-Nb(001) has sustained a 2% contraction and Pd-Nb(110) a 0.5% expansion. If instead, one defines atomic sphere radii for bcc Pd and Nb (the Pd again having been assigned the fcc volume) and defines reference Pd-Nb spacings so that atomic spheres touch, one concludes that Pd-Nb(001) has sustained a 1% contraction and the (110) a 5% contraction. Thus the (110) has sustained either a slight expansion or a significant contraction depending on how the matter is measured. While it has been rather common practice to use touching sphere arguments when discussing adsorbed monolayers on surfaces, it might be argued that for the *bulk* metallically bonded systems of concern here, the volume arguments are more appropriate. Thus, using volume arguments, the (001) Pd-Nb interface [which is more strongly bound than the (110) interface] is contracted, while the (110) shows a weak expansion.

The Ag-Ag spacing, obtained in the equivalent $Ag_xNb_2(110)$ calculation, corresponds to about a 9% atomic-volume contraction. The deformation energy is slight compared with those for Pd, as can be seen from Fig. 5. In the left-hand panel Ag is taken from the undeformed bcc structure, at the fcc atomic volume, to the distorted structure having the Nb(110) planes and the planar spacing obtained from Ag_2Nb_2. The right-hand panel then follows the energy of the system as a function of layer spacing from the Ag_2Nb_2-based value out to a value so that Ag has its fcc atomic volume. All the energies of Fig. 5 are small on the scale of the other terms appearing in Eqs. (1) and (2). It appears that the Ag_2Nb_2-based Ag-Ag separation and associated volume are markedly smaller than those characteristic of bulk Ag. The surfaces of many metallic systems suffer contractions

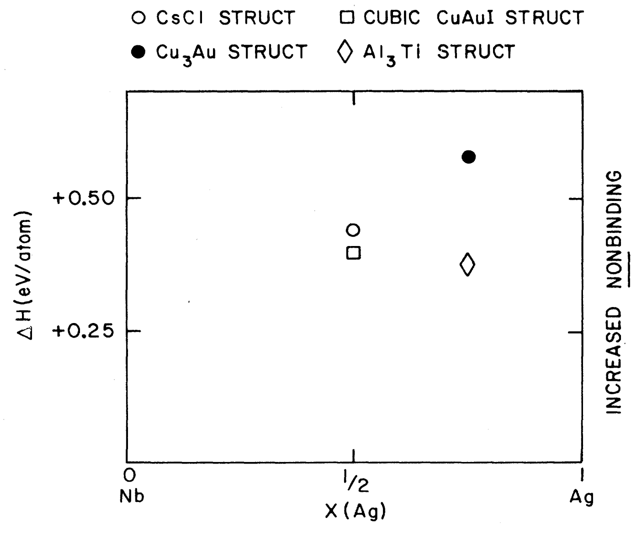

FIG. 4. Calculated heats of formation for some ordered $Ag_xNb_{(1-x)}$ phases. Note that all the heats are nonbinding (i.e., positive).

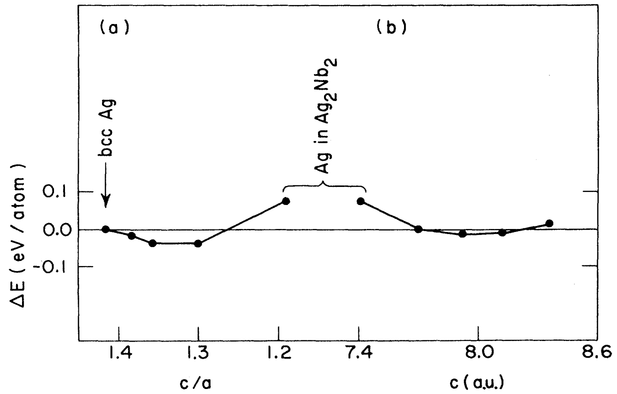

FIG. 5. The binding energy of metallic Ag as a function of distorting it off of the bcc structure (which has been assigned the observed atomic volume of fcc Ag). (a) Orthorhombically distorting bcc Ag so that it has layers with dimensions characteristic of Nb(110) planes, where the separation between layers is the Ag-Ag separation obtained variationally for the $Ag_2Nb_2(110)$ system. (b) The orthorhombic structure with its Nb(110) base planes, where the *c* axis is varied (corresponding to varying the planar separations). The right-hand point corresponds to an atomic volume equal to that of fcc Ag.

of the outermost atomic layer, which is attributable to the layer's lower atomic coordination. A similar effect may be occurring here: the Ag_2 slab does not have vacuum to either side of it in the Ag_2Nb_2 sample but instead has, as will be seen below, ill-bound Nb neighbors.

The top panel of Fig. 6 displays the heat of formation per atom ΔE for the three multilayer systems as a function of multilayer thickness. The (001) Pd-Nb multilayers are still significantly bound at Pd_6Nb_6 while the binding of Pd-Nb(110) has gone to zero by Pd_3Nb_3. These trends are consistent with the experimental situation concerning the adsorption of Pd on Nb, where thick epitaxial layers of Pd form on Nb(001) but only a monolayer on Nb(110). Note that our multilayers involve *two* interfaces in a unit cell, thus the (110) stacks go to zero ΔE with only $1\frac{1}{2}$ layers *to either side of an interface.* The Ag_xNb_x system is nonbinding, consistent with phase-diagram behavior. It should be noted that in the limit of infinitely thick layers,

$$\Delta E \rightarrow \Delta E_{\text{str}}/2 \ , \tag{3}$$

since the interfaces are sparse and half the system is undistorted Nb while the other half is distorted Pd or Ag. The dashed lines of the figure are these asymptotic values and we see that even the thickest of the calculated multilayers is still far from this "thick" regime.

Given ΔE and ΔE_{str}, the interface energy may be estimated:

$$\xi = n(\Delta E - \Delta E_{\text{str}})/2 \ , \tag{4}$$

where, unlike Eq. (2), the n multiplies the right-hand side, since these terms have now been defined per atom. The results are plotted in the bottom panel of the figure. With the possible exception of Pd-Nb(110), these ξ do not appear to have converged to an asymptotic result—though the exact values of the ξ and whether they have a fixed value, as a function of multilayer thickness, depends on a detailed balance of the two terms on the right of the equation. The ξ for Pd-Nb(001) is binding, i.e., ξ is negative, and a factor of more than 2 greater than that for Pd-Nb(110). The less close-packed (001) stacking allows more unlike nearest Pd-Nb neighbor pairs and hence, since these neighbors tend to bond, has the larger interface energy. Since ξ is, in effect, the bonding energy associated with the *pair* of atoms in the interface, while the heats of formation of Fig. 3 are defined per atom, the bonding energy in the Pd-Nb(001) interface is comparable to the heats of the Pd_2Nb and Pd_3Nb compounds and greater than the heats for PdNb. Consistent with bulk phase-diagram behavior, ξ for Ag-Nb is nonbonding and the heats are of the order of the heats obtained for Ag-Nb in Fig. 4. A limited number of calculations have also been done for Ag-Nb(001), yielding a ΔE_{str} which is essentially zero valued and a ξ of $+1.5$ eV per atom pair. For both Ag and Pd on the Nb(001) surface, with more bonds across the interface than on the (110) surface, ξ is larger in magnitude than for the (110) case. While this represents an increase in bonding for Pd, for Ag it represents an increase in *non*bonding, i.e., a larger, more positive ξ.

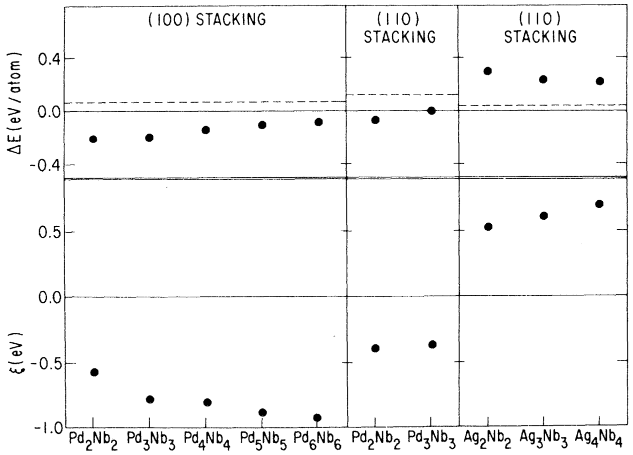

FIG. 6. Top panel: the binding energies, per atom, of $Pd_xNb_x(001)$, $Pd_xNb_x(110)$, and $Ag_xNb_x(110)$ multilayers as a function of multilayer thickness. The dashed lines are the asymptotic ΔE for the limit of infinitely thick multilayers (see text). Bottom panel: ξ, the energy per atom pair in an interface obtained by subtracting the calculated distortion energies ΔE_{str}, for all Pd (or Ag) layers in a multilayer from the multilayer binding energy.

Of all the multilayer systems studied in this paper, only for Pd-Nb(110), which has the smallest interface and the largest distortion terms, does the ΔE_{str} play any substantial role in the energy balance. While the adsorption of Pd on Nb is (surprisingly) well described in terms of these bulk energy terms alone, this is not the case for Ag-Nb. The bulk Ag-Nb terms are consistent with bulk phase behavior, as they ought to be, but are not consistent with the observed Ag adsorption. Thus the surface-energy contribution must play a role, causing Ag to wet Nb rather than clustering. From Fig. 6 it would appear that this term must be substantial.

One measure of the bonding is the charge transfer on or off an atomic site. Values of the change in the total electronic charge for atoms in the layered compounds compared to the charge in the elemental metals are plotted in Fig. 7. The charge transfer is off of Nb and onto Pd and Ag, consistent with electronegativity ideas. The charge transfer is largely associated with the Nb in the interface; those Nb atoms not at the interface suffer little transfer. This contrasts with the Pd and Ag layers, where the charge perturbation penetrates deeper. Larger transfer is seen for Pd-Nb(001) than for the more weakly bound Pd-Nb(110); however, the greatest transfer is encountered in nonbonding Ag-Nb. The transfer associated with the *d*-like component of the charge is plotted in Fig. 8, the most striking feature of which is the near-zero transfer at Pd sites. This is a characteristic of Pd or Pt compound formation: alloying is accompanied by a filling of their "*d* bands" which is accommodated by a hybridization of non-*d* character into the occupied *d*-band states. These *d* bands, with *d* and non-*d* components hybridized into them, are chemically active but with a near-zero net *d* transfer causing a near-zero

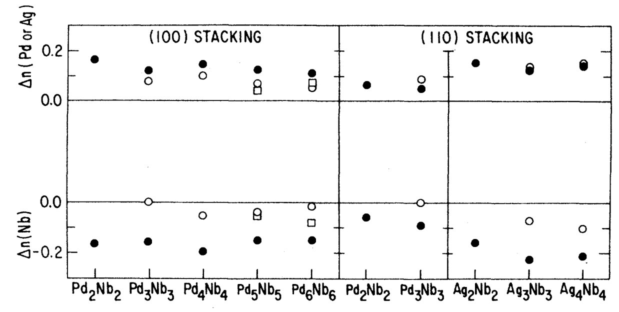

FIG. 7. Charge transfer on (positive Δn) or off (negative Δn) individual atomic sites in the multilayers. Solid circles correspond to atoms in the interface, i.e., in the layer touching the other atomic species; open circles are for the layer adjacent to the interface layer, and the open squares for Pd_5Nb_5 and Pd_6Nb_6 are for those layers furthest removed from the interfaces. The Δn were calculated employing an extrapolation of the charge density from the atomic sphere out to a Wigner-Seitz sphere radius (where Pd, Ag, and Nb were assigned radii reflecting their elemental volumes).

Coulomb shift of the levels. Despite Ag and Nb being more poorly bonded to each other than to themselves, the Ag site Δn and Δn_d are characteristic of what is encountered in noble-metal alloy formation,[13] i.e., the d-electron count drops because of the hybridization of non-d character into the filled d bands and thus d-electron loss is compensated by an even larger increase of non-d character at the Ag site. As a result the net charge transfer is opposite in sign to that of the d. The other case of large Δn_d occurs for the interface Nb sites in Nb-Pd(001), the multilayer undergoing the largest favorable bonding. Here the net and d charge transfer are of the same sign and magnitude. The Δn and Δn_d remain of the same sign, but are smaller in magnitude in Pd-Nb(110), while in nonbonding Ag-Nb(110) there is little change in the interface Nb d count attending the rather substantial net loss in charge. Another measure of the net charge transfer is the chemical shift in core electron energies. This will be discussed in a subsequent paper.

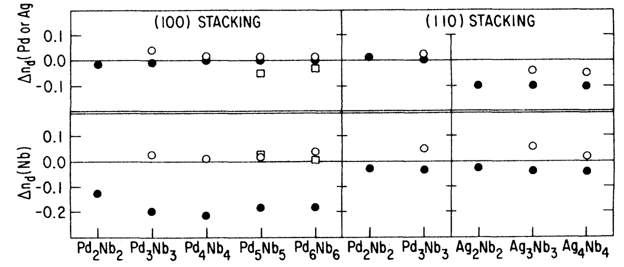

FIG. 8. Δn_d, the d-like component of the charge transfer for individual sites in the multilayers. The calculations and notations follow those of Fig. 5.

Local densities of states $\rho(\varepsilon)$ for the different atomic sites are given for $Pd_6Nb_6(001)$, $Pd_3Nb_3(110)$, and $Ag_3Nb_3(110)$ in Figs. 9, 10, and 11, respectively. To the right of each figure are the densities of states of bcc Nb and of the elemental Pd or Ag metal with the appropriate Nb planar spacing and distance between planes. The elemental Pd(001) and (110) $\rho(\varepsilon)$ are very different from one another and from that of fcc Pd. (When making comparisons between plots, note the changes in vertical scales.) Common among the plots is the tendency for the metal layers furthest from the interfaces to have $\rho(\varepsilon)$ most resembling the elemental behavior.

Consider the Nb $\rho(\varepsilon)$ of Fig. 9. The interface Nb differs from the others in two ways: first, there is a sharp peak ~ 1 eV above the Fermi level ε_F, and second, there is a depletion of states 0–2 eV below ε_F. Both of these features occur in less-pronounced form for the interface Nb in the $Pd_3Nb_3(110)$ of Fig. 10. The peak above ε_F appears as well in surface calculations for bare Nb and for Nb with a monolayer of Pd atop. The peak is associated with having a Nb surface or interface. From Figs. 9 and 10, it appears to be more pronounced with the stronger Pd-Nb bonding of the (001) stacking. The loss in Nb d character in this stacking (cf. Figs. 7 and 8) is related to the depletion in $\rho(\varepsilon)$ just below ε_F. Pd-Nb(110) with its weaker bonding displays a similar, but weaker, depletion.

The interface peaks above ε_F are also seen in the Pd $\rho(\varepsilon)$ of Figs. 9 and 10. From the relative amplitudes of the peaks it is clear that the states are primarily Nb-like although with significant Pd character hybridized in. Vestiges of the peaks are seen for Pd's and Nb's away from the interface: this state is not completely localized at the interface. The more striking feature of the interface Pd's $\rho(\varepsilon)$ is the redistribution of states from just below ε_F in the undisturbed Pd to the middle and lower part of the Pd bands with little, if any, chemical shift in the position of the lower bands. Thus both the Pd and Nb $\rho(\varepsilon)$ show a depletion of states in the same energy region, but the Pd states are shifted downwards while the Nb states are shifted above ε_F. The (bonding-antibonding) hybridization responsible for redistribution of states at the interface is at the root of the Pd-Nb bonding.

The situation is different for the Ag-Nb multilayer where the Nb surface peak is suppressed (a situation also seen in slab calculations) and there is no depletion in the interface Nb $\rho(\varepsilon)$ just below ε_F. Instead there is some buildup in Nb $\rho(\varepsilon)$ in the vicinity of the Ag d band 4–6 eV below ε_F and there is a definite depletion in the density of states 2–4 eV down. Figures 7 and 8 indicate a large drop in Nb interface site charge which, unlike that in the Pd-Nb multilayers, is non-d in character. This would appear to be associated with the depletion 2–4 eV down. The Ag d-band structure 6–8 eV below ε_F seems largely unaffected on going to the interface, while the higher-lying $\rho(\varepsilon)$ has been severely affected, having been largely removed from the same -2–-4 eV region from which the Nb depletion also occurred. Naively, such a redistribution of the density of states would presage substantial Ag-Nb bonding. This increase in Ag-Nb bond-

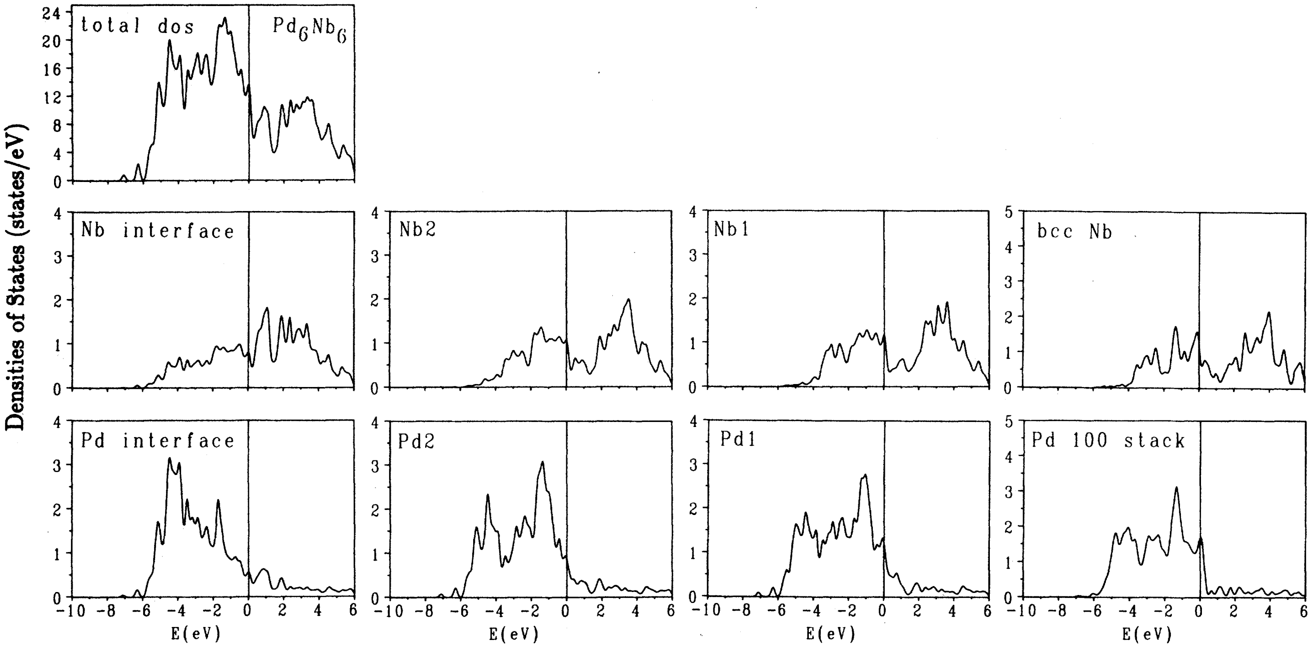

FIG. 9. The total density of states and local densities of states for $Pd_6Nb_6(001)$, where Nb2 refers to Nb's adjacent to the interface Nb's and Nb1 to those Nb's once further removed. The right-hand panels display the density of states of bcc Nb and of Pd constrained to have Nb-like (001) layers and the Pd-Pd separation employed in all the $Pd_xNb_x(001)$ multilayer calculations. The total density of states involves a sampling over all crystal space while the lower panels have their sampling restricted to the charge within the atomic spheres.

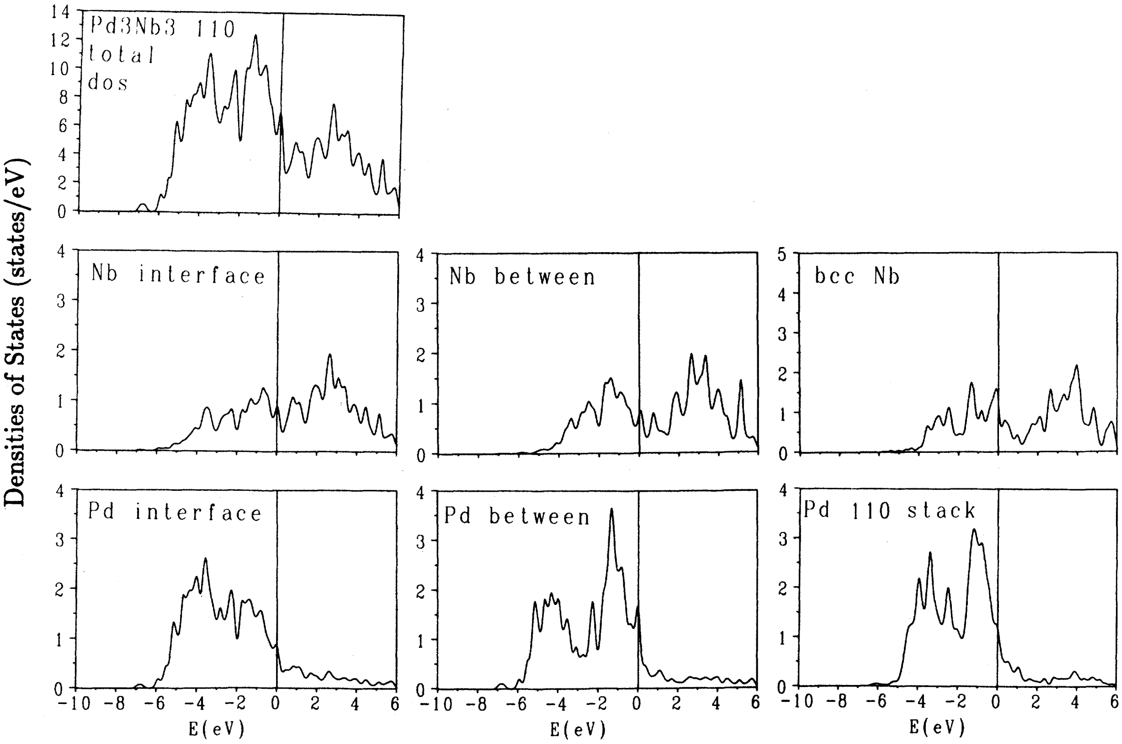

FIG. 10. The total density of states and local densities of states for $Pd_3Nb_3(110)$. See Fig. 9 and the text for further details.

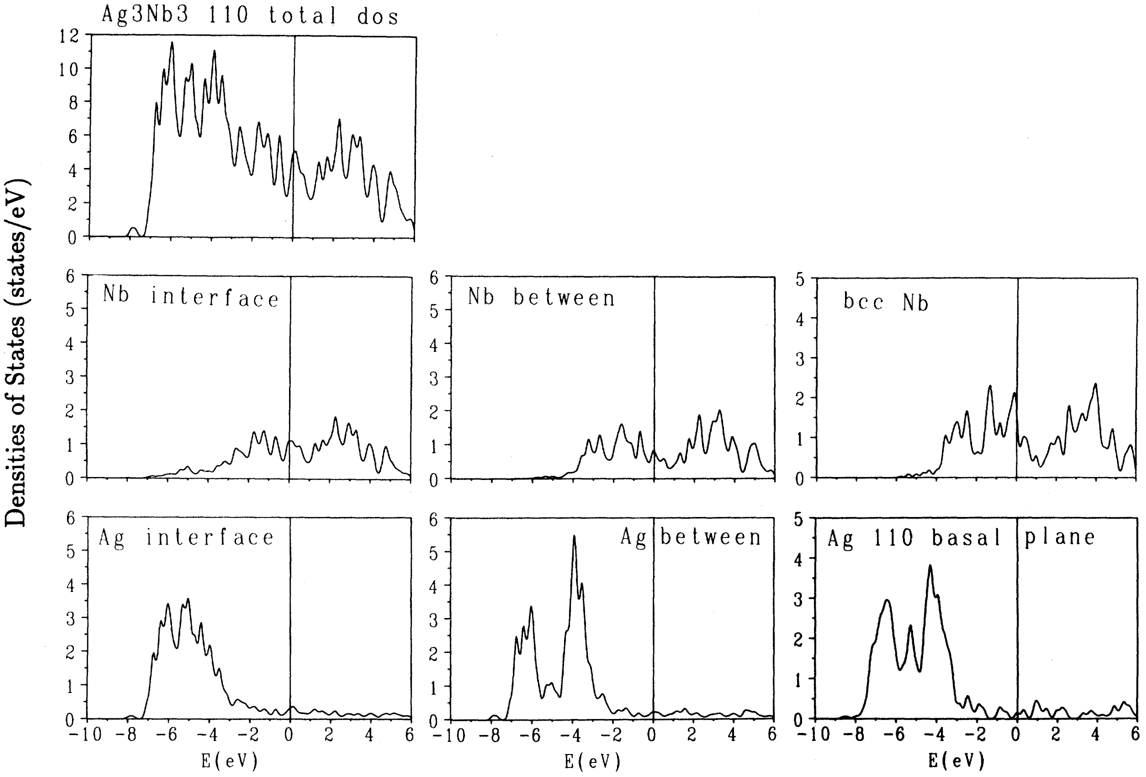

FIG. 11. The total density of states and local density of states for $Ag_3Nb_3(110)$. See Fig. 9 and the text for further details.

ing, however, comes at the expense of Nb-Nb, and to a lesser extent Ag-Ag, bonding energy.[14]

V. SURFACE ENERGIES OF THE LIQUID METALS: IMPLICATIONS

While experimental surface energies are not, as a rule, available for specific crystal faces, they do exist[12] for the liquid metals tabulated as a function of surface area. Assuming atomic densities appropriate to the (001) and (110) planes of Nb, one obtains the surface energies per atom given in Table I. The range in $\gamma(\mathrm{Nb})$ reflects the range in quoted experimental values.

Inspection of Fig. 4 shows that in the case of Ag-Nb(110), the wetting of Nb by Ag is not favored, due to the interface and deformation terms, by an amount of ~ 0.7 eV per atom. The difference in γ_L between Ag and Nb indicates a lowering in surface energy of ~ 0.5 eV per atom by having a Ag rather than Nb surface. This energy gain is not quite enough to cancel the interface energy but is so close as to suggest that a more careful accounting of the reduction in surface energy associated with adsorbing Ag of Nb might compensate the unfavorable Ag-Nb bonding. It will be seen that the liquid γ_L underestimate the γ appropriate to crystalline faces. The surface calculations of the next section will address this issue.

Even though the ξ and ΔE_{str} terms alone appear to provide a satisfactory description of the adsorption energetics of Pd on Nb (001) and (110), the difference in $\gamma_L(\mathrm{Nb})$ and $\gamma_L(\mathrm{Pd})$ suggests that the surface-energy difference of Eq. (1) is of significance here as well. Furthermore, if the surface-energy difference encourages the adsorption of Ag and Pd on Nb, it discourages the wetting of Nb on Pd and Ag. From the magnitudes of the heats of formation obtained for the Pd-Nb compounds, we would predict that adsorbing Nb on Pd will lead to compound formation rather than layer-by-layer growth. Experimentally[15] compound formation for Nb on Pd appears to be the case. The skewing of the heats (see Fig. 3) suggests that Pd-rich compounds will likely be formed.

VI. RESULTS: ELEMENTAL CRYSTALLINE SURFACE ENERGIES

Calculated surface energies for various faces of crystalline Nb, Ag, and Pd appear in the first columns of Table II. As discussed in Sec. II, both the energy per atom in

TABLE I. Liquid-metal surface energies in eV/atom assuming atomic densities appropriate to the Nb(110) and Nb(001) surfaces.

	Nb(110)	Nb(001)
$\gamma_L(\mathrm{Ag})$	0.44	0.63
$\gamma_L(\mathrm{Pd})$	0.71	1.00
$\gamma_L(\mathrm{Nb})$	0.91–0.96	1.29–1.36

TABLE II. Surface energies γ.

Surface	Present calculations γ (eV/atom)	Present calculations γ (J/m^2)	Smith and Banerjea[a] γ (eV/atom)	Tyson and Miller[b] γ (J/m^2) $T=0$	Mezey and Giber[c] γ (J/m^2) $T=0$	Expt.[d] γ (J/m^2)	Liquid metal γ (J/m^2)
Nb(110)	1.4	2.9		2.65	3.10	2.44, 2.8, 1.5(001), 1.4(110), 4.9(001), 5.0(110)	1.90
(001)	2.1	3.1					
Ag(001)	0.7	1.3	0.85	1.24	1.38	1.32,[b] 1.54	0.92
(110)	1.0	1.4	1.13				
Pd(001)	1.1	2.3					
(110)	1.7	2.5		2.00	2.17		1.47

[a] Reference 16.

[b] Polycrystalline, Ref. 17.

[c] Polycrystalline, Ref. 18.

[d] Polycrystalline, unless otherwise noted, Ref. 19.

the bulk and surface energy γ were derived from the total energies calculated for varying slab thicknesses. The second set of results are theoretical estimates[16] also based on local density theory for Ag and are in reasonable accord with our results. The next two sets of results may be deemed semiempirical in nature: Tyson and Miller estimated[17] crystalline γ based on liquid surface tension data while Mezey and Giber made estimates[18] based on enthalpies of atomization. For the most part, the experimental results[19] are not obtained much more directly than the semiempirical estimates. Where appropriate, all these results are corrected to zero temperature,[17] to which the present results are appropriate.

The various estimates are in semiquantitative agreement with one another and with experiment. (The scatter in the estimates is less than that in the experiments.) The liquid metal γ are markedly smaller than the crystalline values as might be expected since they are, in effect, high-temperature values.[17]

The calculations show the closer-packed crystalline faces to have the smallest γ as expected from simple bond-cutting arguments. While clearly such arguments are not correct in detail, it is still of interest to see whether the physical trends can be understood in a simple—perhaps oversimplified—physical picture. Creating a close-packed surface involves the loss of fewer nearest neighbors than does creating a more open surface. Viewing γ as the energy cost associated with the loss of bonding at the surface, γ should scale with the number of bonds cut when creating the surface. For the fcc lattice, a (001) surface involves the loss of 4 of 12 nearest neighbors, while a (110) surface involves the loss of 5 of 12 nearest neighbors. Thus, to first approximation, one expects $\gamma(110)$ to be $\frac{5}{4}\gamma(001)$ and this is roughly so.

Consideration of the bcc lattice is complicated by the question of whether one counts the eight closest neighbors alone or the six additional slightly further neighbors as well. Thus, forming a (001) surface involves the loss of 4 of 8 (or 5 of 14) nearest neighbors, while for a (110) surface there is a loss of 2 of 8 (or 4 of 14). For Nb, $\gamma(001)/\gamma(110)$ lies between $\frac{4}{2}$ and $\frac{5}{4}$, consistent with the view that the six slightly further neighbors also make an important, though weaker, bonding contribution.

Our results for γ show less variation between faces, on the order of 10%, when considered per unit area. This is the appropriate choice of units when considering equilibrium crystal shapes, etc. If there were no face dependence in γ, i.e., jellium, then the equilibrium crystal shape would be a sphere because this would minimize the surface area and hence the total surface energy. Since the majority of elements do grow rather spherically, we would expect only small variations in energy per unit area. When comparing to bulk properties such as heats of formation, however, energy per atom is a more useful number.

The small variation with crystal face in γ given per unit area can also be rationalized in terms of bond cutting since the area per atom and the number of cut bonds are (inversely) proportional. In all the cases that we have considered, the closer-packed surface also has the lower γ per unit area as one would expect when the directional bonding is included. [Our results in this respect disagree with Smith and Banerjea[16] for the case of Ag. For Nb, experiment[19] is inconsistent as to whether the (001) or (110) face has the larger or smaller γ per unit area; our results are consistent with the naive expectation.] While it is likely that most elemental systems will behave in this manner, there could be exceptions, especially in the case of compounds.

VII. RESULTS: ADHESION ENERGIES OF Pd AND Ag ON Nb

Total energies E_T and densities of states have been obtained from monolayers of Pd and Ag on either side of slabs of Nb. The densities of states will be reported elsewhere, where the spectroscopic behavior of such systems will be considered. These densities of states distinctly resemble those seen for the bulk multilayer with their interface states just above the Fermi level. It is useful to define an adhesion energy ΔE_A, which is the difference in energy between a Nb surface covered by a monolayer of M (Pd or Ag) and a bare Nb surface plus a ball of bulk metal M whose energy is characteristic of an atom M immersed in the bulk, i.e., neglecting the (positive) surface energy of M. This quantity is

$$\Delta E_A \equiv \tfrac{1}{2}E_T(M/\mathrm{Nb}) - [\tfrac{1}{2}E_T(\mathrm{Nb}) + E(M)] , \quad (5)$$

where the slab total energies E_T have been multiplied by $\frac{1}{2}$ since a slab has two surfaces, each with (or without) an adlayer of atom M. The E_T are defined for a unit cell of the slab involving a single column of atoms, and $E(M)$ is the total energy per atom in bulk M. Similar to Eq. (1), one may define a surface energy associated with metal M adsorbed on Nb, namely

$$\begin{aligned}\gamma(M/\mathrm{Nb}) &\equiv \tfrac{1}{2}E_T(M/\mathrm{Nb}) - \frac{n}{2}E(\mathrm{Nb}) - E(M) \\ &\quad - \xi - \Delta E_{\mathrm{str}} \\ &= \Delta E_A + \gamma(\mathrm{Nb}) - \xi - \Delta E_{\mathrm{str}} , \quad (6)\end{aligned}$$

where n is the number of Nb layers in the slab. Both ΔE_A and $\gamma(M/\mathrm{Nb})$ are reported in Table III.

The ΔE_A listed in Table III are all negative, implying that it is energetically more favorable to cover Nb with a monolayer of Pd or Ag than it is to have the bare Nb surface plus a lump of bulk Pd or Ag. (Including the surface energy of the metal ball would make adhesion even more favorable.) The adhesion energies for the Ag and Pd on the two different Nb faces show only a small variation per unit area. As discussed above, such a small face dependence is expected if the adsorption process is one of finding equilibrium crystal shapes. That this argument is appropriate in the case when there are additional constraints on the system such as crystal orientation is not clear *a priori*. That the results do indeed show only a small variation between faces suggests that for monolayer coverages, at least, Ag and Pd will grow uniformly and pseudomorphically on free Nb particles.

For Ag and Pd on the Nb(110) substrate, as well as for Ag/Nb(001), the $\gamma(M/\mathrm{Nb})$'s of Table III are smaller than the corresponding $\gamma(M)$'s of Table II. For Pd/Nb(001), however, $\gamma(M/\mathrm{Nb})$ is larger than that for pure Pd. Naively one might expect that $\gamma(M/\mathrm{Nb})$ and $\gamma(M)$ should be equal; in the limit of infinitely thick coverages, this must be true. These differences between $\gamma(M)$ and $\gamma(M/\mathrm{Nb})$ are associated in part with the fact that the surfaces here involve only a monolayer of Pd or Ag in a geometry which is different than the surfaces of elemental Pd or Ag. There is, of course, no reason that the energy terms of Eq. (6) must yield the elemental surface energy at monolayer coverage and we would be surprised if indeed they were the same. Nevertheless, it is interesting to note that to bring $\gamma(M/\mathrm{Nb}(110))$ into line with the elemental metal values requires substantially larger and more negative ξ's than appear in Fig. 6. In the case of Pd-Nb(110) this would require values which would then be somewhat larger than the heats of formation calculated for the ordered Pd-Nb(110) compounds; Ag-Nb(110) would require a negative ξ, i.e., bonding at the interface, contrary to the bulk phase diagram. The small value of $\gamma(\mathrm{Ag/Nb}(001))$ is due mainly to the large and positive (1.5 eV) interface energy. The reason that the magnitude of ξ is larger for Ag of Nb(001) than on Nb(110) is again the same as for Pd, i.e., the number of unlike neighbors, but now the term is nonbinding.

From Eq. (6) we can define a difference surface energy as

$$\begin{aligned}\Delta\gamma_M &= \gamma(M/\mathrm{Nb}) - \gamma(M) \\ &= \Delta E_A + [\gamma(\mathrm{Nb}) - \gamma(M)] - \xi - \Delta E_{\mathrm{str}} . \quad (7)\end{aligned}$$

Since $\Delta E_{\mathrm{str}} \geq 0$ and $\Delta E_A < 0$ [necessary for a smooth interface and thus for $\gamma(M/\mathrm{Nb})$ to be defined], these terms will always favor $\Delta\gamma_M < 0$. For M=Ag,Pd, the difference in elemental surfaces energies give a positive contribution to $\Delta\gamma_M$. The difference between Ag and Pd is the sign of ξ: the nonbinding of Ag forces $\Delta\gamma_M$ negative, while for Pd, ξ increases the positive difference in effective surface energies of the adlayer versus the pure material. Thus it is not surprising that $\Delta\gamma_{\mathrm{Ag}} < 0$ for both Nb substrates. For Pd, the difference in ξ between the two substrates accounts for the difference in $\Delta\gamma_{\mathrm{Pd}}$; the significantly larger ξ of Pd-Nb(001) compared to Pd-Nb(110) (-1.3 versus -0.8 J/m^2), as well as the smaller distortion energies for Pd/Nb(001) (0.2 versus 0.5 J/m^2), make $\Delta\gamma_{\mathrm{Pd/Nb(001)}} > 0$. These values of $\Delta\gamma_M$ have implications for multilayer growth. As was discussed earlier, if the substrate's surface energy is greater than the adlayer's, then the surface terms will favor wetting of the surface. Similarly, we can ask what happens when the first adlayer is complete and more atoms are adsorbed: will this layer now wet? For the second layer, $\xi \equiv 0$ in the simplest approximation, since now the bonding is to like atoms. The adsorption energy of the second layer, ΔE_2, should be approximately

TABLE III. Calculated adhesion and "surface" energies for adsorbed monolayers on Nb. (The conversion between eV/atom and J/m^2 was done before rounding either value; the apparent inconsistencies of the values in different units are due to rounding to the precision shown.)

	Adhesion energy ΔE_A		Surface energy for adlayer, $\gamma(M/\mathrm{Nb})$	
Surface	eV/adatom	J/m^2	eV/adatom	J/m^2
Ag/Nb(110)	-0.3	-0.5	0.4	0.8
Pd/Nb(110)	-0.7	-1.4	0.9	1.9
Ag/Nb(001)	-0.4	-0.6	0.2	0.3
Pd/Nb(001)	-0.9	-1.3	2.0	2.9

$$\begin{aligned}\Delta E_2 &= \gamma(M+M/\mathrm{Nb})-\gamma(M/\mathrm{Nb})+\Delta E_{\mathrm{str}}\\ &\approx \gamma(M)-\gamma(M/\mathrm{Nb})+\Delta E_{\mathrm{str}}\\ &= -\Delta\gamma_M+\Delta E_{\mathrm{str}}\ .\end{aligned} \tag{8}$$

This equation predicts that Pd/Nb(110), Ag/Nb(110), and Ag/Nb(001) should form only a single adlayer, since $\Delta E_2>0$ ($\Delta\gamma_M<0$), whereas for Pd/Nb(001), $\Delta E_2<0$, and thus more layers could wet. This trend is in agreement with the experimental results. For $\Delta E_2>0$, we do not expect wetting, but rather other behavior, such as compound formation or clustering, depending on the details of the system. It is clear that Eq. (8) is an oversimplification, since only two layers would ever wet if it were strictly valid, since $\Delta E_{\mathrm{str}}>0$. [If $\Delta E_{\mathrm{str}}=0$ and $\gamma(M)\le\gamma(M/\mathrm{Nb})$, then infinitely thick layers would be possible.] What has been neglected is the fact that ξ (cf. Fig. 6), as well as the surface energy, is layer dependent. The only case for which ξ is approximately layer independent, and thus satisfies the conditions of Eq. (8), is Pd/Nb(110), where experimentally only one layer adsorbs epitaxially, consistent with our calculations. For Pd/Nb(001) it is likely that ξ will give an additional contribution favoring thick multilayer formation. Thus we see that the experimentally observed adlayer behavior is an interplay of surface and bulk properties.

VIII. DISCUSSION

In this paper we have considered the energetics of Pd-Nb and Ag-Nb multilayer and adlayer formation. The possibilities have not been completely explored since neither incommensurate multilayers nor adlayers were addressed. Nonetheless, dividing the energetics into distortion, interface, and surface-energy contributions allows one to draw conclusions and make predictions. For example, although the distortion energy is smaller in magnitude than the other terms, its magnitude provides important clues concerning the tendency towards pseudomorphic growth. We find $0<\Delta E_{\mathrm{str}}$ [Ag:Nb(110)] $<\Delta E_{\mathrm{str}}$[Pd:Nb(001)] $<\Delta E_{\mathrm{str}}$[Pd:Nb(110)]. Since ΔE_{str} is an energy cost, we would expect that experimentally the tendency to have incommensurate adlayers increases along this sequence. This appears to be the case.

Combining the surface- and interface-energy contributions with the heats of formation of some ordered compounds allows further predictions to be made. Surface-energy considerations encourage Pd and Ag to cover a Nb substrate. While we have not done calculations for Nb covering either Pd or Ag, we can anticipate the result: Nb will tend not to wet an Ag surface, and will be more likely to form compounds than to cover Pd monatomically. In making these statements, we presume that the surface-energy loss associated with forming an energetically favorable compound would be preferable to the loss associated with covering Pd with pure Nb. From Fig. 3 one would expect these compounds to be Pd-rich, provided the kinetics of atomic rearrangement at the surface allow it.

The results seen for bulk Pd-Nb compounds in Fig. 3 are at first glance surprising in that the heats are heavily skewed in favor of having Pd-rich compounds. Naively one might expect to have the largest binding at 50%-50% concentration, where one can maximize the number of unlike nearest-neighbor atom pairs. This skewing has been seen in calculations[20] for Pd alloyed with Ti, Zr, and Hf as well and appears to be associated with having the Pd d bands filled upon alloying. Once filled, these bands may float free of the Fermi level so as to maximize the bonding. This filling occurs when Pd is in the majority by as much as a 3:1 factor and its effect on the heat of formation is even more pronounced than at 50%-50% concentration.

Densities of states for the multilayers were considered in Figs. 9–11. As already discussed, distinct features of the bonding are illustrated particularly when taken with the charge-transfer counts Δn and Δn_d. One notable feature is the Nb-like peak which lies $1-1\frac{1}{2}$ eV above the Fermi level in what is a hollow in the density of states for bulk bcc Nb. The local densities of states indicate that it is an interface state largely localized on the Nb and Pd (or Nb and Ag) interface atoms. This feature is most pronounced for the Pd/Nb(001) multilayer, less for Pd/Nb(110), and least for Ag/Nb(110), i.e., it is most pronounced when the interface binding ξ is greatest. Although not displayed here, this peak also appears in the densities of states for adlayers of Ag or Pd on Nb surfaces and it has been seen experimentally.[21] This feature is also present[21] for the bare Nb surface, though less strongly localized than for the adlayers. As expected for the shift of an unoccupied "antibonding" state, the peak is chemically shifted by $\sim\frac{1}{2}$ eV further above the Fermi level on going from bare Nb to an interface. These interface states can be important to the binding of an interstitial atom, such as H or B, at an interface or grain boundary as well as to the binding of an atom or molecule to the surface of Nb with or without a metal adlayer such as Pd.

We have also estimated surface energies for several crystal faces of Nb, Ag, and Pd, where we reaffirm the expectation that the close-packed surfaces have the smaller surface energies whether measured per atom or per unit area. The smaller γ can be understood simply by the fact that forming a close-packed surface breaks fewer bonds than a more open one. The small variation in γ per unit area can be rationalized both in these terms as well as small perturbations on the jellium model of metals, implying that Ag, Pd, and Nb will all have rather spherical equilibrium crystal shapes. It should be noted that the agreement between the various *a priori* and semiempirical estimates of γ is better than the agreement among the various experimental values.

By considering two transition-metal systems with different types of bulk phase diagrams, the strong compound-forming Pd-Nb system, and the complete immiscibility of Ag-Nb, we have shown that the surface-energy terms can strongly modify the energetics of adlayer adsorption to the extent of giving behavior apparently in disagreement with the bulk phase diagram. This interplay of surface and bulk terms is important in determining the growth of multilayer and adlayer metal-

metal materials. For a system in which the dominant attractive term is the bulk interface energy [Pd/Nb(001)] and is comparable to bulk heat of formation (strong compound formation), it is not surprising that the energetics can be described reasonably well by bulk terms alone. For the cases when the difference in surface energies is of the same scale or larger than the other bulk contributions (weak compound formation), a detailed accounting of surface terms is essential in order to describe the adlayer behavior.

Finally, we comment on what conditions are favorable to multilayer formation. From the results of this paper, it is clear that in order to form coherent multilayers (superlattices), one would like to use materials with nearly equal surface energies and small distortion energies. If either of these energies is large, pseudomorphic growth of at least one of the two interfaces (M_1/M_2 or M_2/M_1) will be suppressed. Likewise, to avoid interdiffusion of the metals at the interface, the interface energies should not be too large or heavily skewed. Not surprisingly, the condition that the surface energies are approximately equal means that the bulk phase diagram will govern both the overall energetics (as it must, since the multilayers are bulk systems) as well as the layer-by-layer growth. Thus, good systems for growing multilayers are those in which the surface contributions to the energetics are minimized and the growth can be understood from the bulk properties.

ACKNOWLEDGMENTS

We thank L. Q. Jiang, P. D. Johnson, and M. Strongin for helpful discussions. This work was supported by the Division of Materials Sciences, U.S. Department of Energy, under Contract No. DE-AC02-76CH00016.

---

[1] G. Kellog (unpublished).

[2] M. J. Sagurton, M. Strongin, F. Jona, and J. Colbert, Phys. Rev. B **28**, 4075 (1983).

[3] M. W. Ruckman and L. Q. Jiang, Phys. Rev. B **38**, 2959 (1988); J. Tranquada and P. D. Johnson (unpublished).

[4] J. W. Davenport, Phys. Rev. B **29**, 2896 (1984).

[5] R. E. Watson, M. Weinert, and J. W. Davenport, Phys. Rev. B **35**, 9284 (1987).

[6] When calculating the relative stability of two phases, one is taking the difference in total energies and it is important to obtain those total energies with a common set of approximations. One shortcoming of the muffin-tin approximation is, of course, the description of the potential in the interstitial region between the atomic spheres (which we require to be nonoverlapping). In an attempt to minimize any adverse impact of the approximations, we employ a common atomic-sphere radius (for any given element) in the several total-energy calculations. This works well when calculating or comparing calculated heats of formation for transition-metal compounds. However, there are problems when considering the relative stability of the fcc versus the bcc phase in the noble metals. Taking the two phases at equal atomic volumes, the atomic packing in the bcc structure is such that smaller nonoverlapping atomic spheres can be accommodated than is the case in the fcc. Using a common sphere radius causes the bcc total energy to be slightly better bound for Au (see Ref. 7), while using different-sized touching spheres in the two structures leads to the fcc being better bound by a more substantial amount. Comparison with calculations for other transition metals suggest that a more rigorous treatment of the crystal potential within the local-density approximation would yield the Au fcc structure being the better bound by several hundredths of an eV/atom. For silver, calculated at the observed metallic volume, calculations with common spheres indicate the bcc to be stabler by 0.02 eV/atom while with touching spheres the fcc is stabler by 0.07 eV/atom with a reasonable accounting of muffin-tin effects leaving the fcc stabler by a value somewhere between. This energy difference is small and its exact value is not important to the energy considerations of this paper.

[7] J. W. Davenport, R. E. Watson, and M. Weinert, Phys. Rev. B **32**, 4883 (1985).

[8] R. E. Watson, J. W. Davenport, and M. Weinert, Phys. Rev. B **34**, 8421 (1986); **35**, 508 (1987); **36**, 6396 (1987).

[9] E. Wimmer, H. Krakauer, M. Weinert, and A. J. Freeman, Phys. Rev. B **24**, 864 (1981); M. Weinert, E. Wimmer, and A. J. Freeman, *ibid.* **26**, 4571 (1982).

[10] See, e.g., Ref. 5.

[11] W. G. Mofatt, *The Handbook of Binary Phase Diagrams* (Genium, Schenectady, New York).

[12] *Handbook of Chemistry and Physics,* edited by R. C. Weist (CRC, Boca Raton, 1985).

[13] An early experimental example of this being R. E. Watson, J. Hudis, and M. L. Perlman, Phys. Rev. B **4**, 4139 (1971).

[14] It is important to realize that the interface energies and heats of formation are always given relative to the reference systems. If we write the total heat of formation ΔH in terms of the cohesive energies E^{coh} (all assumed negative) of the pure materials and the compound, $\Delta H = E_{AB}^{\mathrm{coh}} - E_A^{\mathrm{coh}} - E_B^{\mathrm{coh}}$. Bonding requires $\Delta H < 0$ or $|E_A^{\mathrm{coh}} + E_B^{\mathrm{coh}}| < |E_{AB}^{\mathrm{coh}}|$. The difference between Ag-Nb and Pd-Nb is not the sign of E_{AB}^{coh}, but rather the magnitude relative to the sum of E_A^{coh} and E_B^{coh}. While the interface densities of states changes are a measure of E_{AB}^{coh} and naively suggest substantial Ag-Nb bonding, the total $\Delta H > 0$, consistent with the bulk phase diagram.

[15] L. Q. Jiang (private communication).

[16] J. R. Smith and A. Banerjea, Phys. Rev. Lett. **59**, 2451 (1987), and references therein.

[17] W. R. Tyson and W. A. Miller, Surf. Sci. **62**, 267 (1977); see this for a discussion of the temperature dependence of γ.

[18] L. Z. Mezey and J. Giber, Jpn. J. Appl. Phys. **21**, 1569 (1982).

[19] H. Wawra, Z. Metallkd. **66**, 395 (1975), and references therein; in particular, Y. G. Avraamov and A. G. Gwocdev, Fiz. Met. Metalloved. **23**, 405 (1967), and M. H. Richman, Brown University Technical Report No. At(30-1)-2394-25 1967 (unpublished).

[20] R. E. Watson, M. Weinert, J. W. Davenport, and G. W. Fernando, Phys. Rev. B **39**, 10 761 (1989).

[21] X. Pan, P. D. Johnson, M. Weinert, R. E. Watson, J. W. Davenport, G. W. Fernando, and S. L. Hulbert, Phys. Rev. B **38**, 7850 (1988).